Science Translational Medicine
AAAS

www.sciencetranslationalmedicine.org/cgi/content/full/7/313/313ra182/DC1

# Supplementary Materials for

## Analysis of *ESR1* mutation in circulating tumor DNA demonstrates evolution during therapy for metastatic breast cancer

Gaia Schiavon, Sarah Hrebien, Isaac Garcia-Murillas, Rosalind J. Cutts, Alex Pearson, Noelia Tarazona, Kerry Fenwick, Iwanka Kozarewa, Elena Lopez-Knowles, Ricardo Ribas, Ashutosh Nerurkar, Peter Osin, Sarat Chandarlapaty, Lesley-Ann Martin, Mitch Dowsett, Ian E. Smith, Nicholas C. Turner*

*Corresponding author. E-mail: nicholas.turner@icr.ac.uk

Published 11 November 2015, *Sci. Transl. Med.* **7**, 313ra182 (2015)
DOI: 10.1126/scitranslmed.aac7551

**This PDF file includes:**

Fig. S1. *ESR1* LBD digital PCR assays are sensitive and highly reproducible.
Fig. S2. Patients with *ESR1* mutation have poor outcome on subsequent AI therapy.
Fig. S3. A theoretical model explains the evolution of *ESR1* mutations during treatment for metastatic breast cancer.
Table S1. Clinical and pathological characteristics of the series of patients with advanced cancer.
Legend for table S2
Table S3. Ion AmpliSeq Breast Cancer driver and focal mutation gene panel.

**Other Supplementary Material for this manuscript includes the following:**
(available at www.sciencetranslationalmedicine.org/cgi/content/full/7/313/313ra182/DC1)

Table S2. *ESR1* mutations analyzed and experimental conditions (provided as an Excel file).

**Analysis of *ESR1* mutation in circulating tumor DNA demonstrates evolution during therapy for metastatic breast cancer**

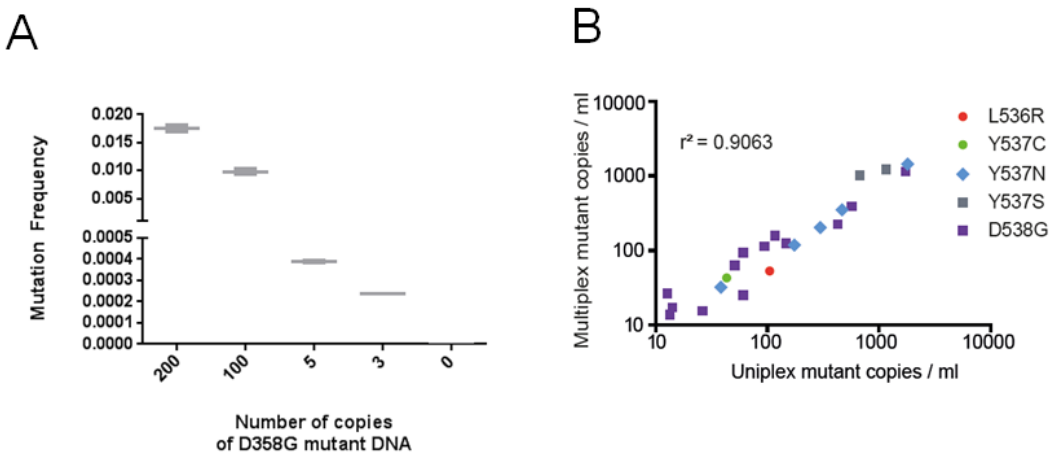


**Figure S1. *ESR1* LBD digital PCR assays are sensitive and highly reproducible.**

A. Limit of detection for D538G assay on mutant DNA. 200, 100, 5, and 3 copies of *ESR1 c.1613A>G* (D538G) DNA were spiked into 15,000 genomes of CAMA-1 DNA, and the number of copies was plotted against the frequency of mutation detected by the assay to show that this assay can detect down to 3 copies in an excess of WT DNA (0.00024 mutant frequency). No positive droplets were detected when CAMA-1 DNA had not been spiked with mutant DNA.

B Correlation of mutational abundance (mutant copies per ml of plasma) between multiplex and uniplex assays in *ESR1*-mutant plasma samples r2=0.90; Pearson's correlation coefficient.

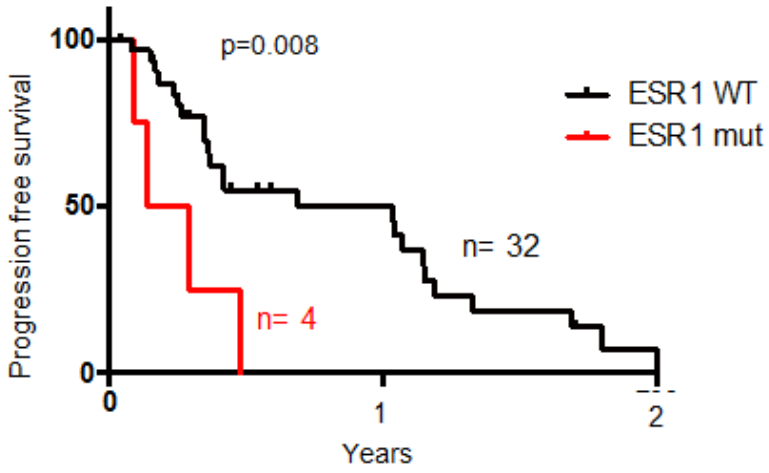


**Figure S2. Patients with *ESR1* mutation have poor outcome on subsequent AI therapy.** Progression-free survival on AI-based therapy after *ESR1* mutation testing for patients with *ESR1* mutant and wild-type (HR 3.711, p=0.008 log rank test). Only patients treated with AI started immediately after disease progression are included.

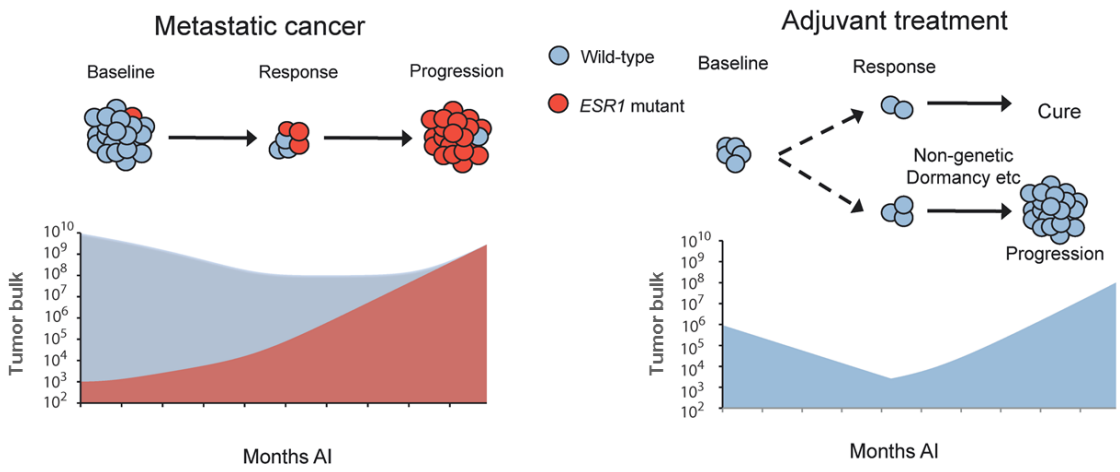


**Figure S3. A theoretical model explains the evolution of *ESR1* mutations during treatment for metastatic breast cancer.** *Left*. In metastatic breast cancer, rare *ESR1* mutant sub-clones exist before therapy, reflecting greater genetic diversity of bulk metastatic cancer, and *ESR1*-mutant subclones grow out under the selective pressure of AI therapy. *Right*. In early breast cancer, AIs treat micro-metastatic disease at substantially lower tumor bulk. *ESR1* mutant sub-clones are not present, and micrometastatic disease is either eradicated by AI therapy or alternative mechanisms of resistance result in relapse. Our data suggest that AI exposure in the adjuvant setting rarely results in selection of *ESR1* mutation as the mechanism of resistance. Once a cancer has developed resistance to AI in the adjuvant setting, further therapy in the metastatic setting is less likely to result in the selection of *ESR1* mutations. If the cancer is resistant to AI therapy, there may be no selective advantage, or less selective advantage, to an *ESR1* mutant subclone during therapy. If a cancer relapses many years after stopping adjuvant AI, then the bulk tumor may remain AI sensitive and there may now be potential to select out an *ESR1* mutant subclone.

**Table S1. Clinical and pathological characteristics of the series of patients with advanced cancer.**

| | |
|---|---|
| n | 171 |
| **Median age** | 58 (24-86) |
| **Tumor subtype** | |
| ER + HER2 - | 107 |
| ER + HER2 + | 19 |
| ER - HER2 + | 17 |
| TNBC | 26 |
| **Grade** | |
| 1 | 9 |
| 2 | 75 |
| 3 | 75 |
| **Visceral disease %** | 64% (108/168) |
| **Bone disease %** | 63% (105/168) |
| **Adjuvant therapy** | |
| Prior adjuvant tamoxifen | 42% (71/171) |
| Prior adjuvant AI | 30% (52/171) |
| Prior adjuvant chemo | 55% (93/169) |
| Prior trastuzumab | 20% (33/169) |
| **Prior metastatic therapy** | |
| Median courses chemo | 0 (range 0-3) |
| Median endocrine (ER+ only) | 1 (range 1-5) |

**Table S2. *ESR1* mutations analyzed and experimental conditions (provided as an Excel file).** List of mutations analyzed in this study, with sequences and concentrations of the corresponding primers and probes for the digital PCR assays (uniplex and multiplex) and list of mutant synthetic oligonucleotides used with corresponding sequences. All ddPCR assays were run at the same conditions (annealing / extension temperature 60°C and 40 cycles of amplification).

**Table S3. Ion AmpliSeq Breast Cancer driver and focal mutation gene panel.**

| | |
|---|---|
| *AKT1* ex4 | *MAP3K1* |
| *BRAF* ex15 | *PIK3CA* ex5, 8, 9, 20 |
| *CDH1* | *PIK3R1* ex4, 6 |
| *GATA3* | *PTEN* |
| *KIT* ex11 | *RUNX1* ex1, 2, 3 |
| *KRAS* ex2 | *SF3B1* ex14, 15 |
| *MAP2K4* | *TP53* ex5, 6, 7, 8 |